Chinese Chemical Letters 36 (2025) 110222

Contents lists available at ScienceDirect

Chinese Chemical Letters

journal homepage: www.elsevier.com/locate/cclet

A portable and versatile fluorescent platform for high-throughput screening of toxic phosgene, diethyl chlorophosphate and volatile acyl chlorides

Beitong Zhu[a,1], Xiaorui Yang[a,1], Lirong Jiang[b,*], Tianhong Chen[c,*], Shuangfei Wang[a], Lintao Zeng[a,*]

[a] Guangxi Key Laboratory of Clean Pulp & Papermaking and Pollution Control, School of Light Industry and Food Engineering, Guangxi University, Nanning 530004, China
[b] School of Chemistry and Chemical Engineering, Guangxi Minzu University, Nanning 530006, China
[c] College of Chemistry, Beijing Normal University, Beijing 100875, China

ARTICLE INFO

Article history:
Received 26 May 2024
Revised 2 July 2024
Accepted 5 July 2024
Available online 6 July 2024

Keywords:
Fluorescent platform
High throughput
BODIPY
Linear discriminant analysis
Phosgene
Acyl chloride
Diethyl chlorophosphate

ABSTRACT

Highly toxic phosgene, diethyl chlorophosphate (DCP) and volatile acyl chlorides endanger our life and public security. To achieve facile sensing and discrimination of multiple target analytes, herein, we presented a single fluorescent probe (**BDP-CHD**) for high-throughput screening of phosgene, DCP and volatile acyl chlorides. The probe underwent a covalent cascade reaction with phosgene to form boron dipyrromethene (BODIPY) with bright green fluorescence. By contrast, DCP, diphosgene and acyl chlorides can covalently assembled with the probe, giving rise to strong blue fluorescence. The probe has demonstrated high-throughput detection capability, high sensitivity, fast response (within 3 s) and parts per trillion (ppt) level detection limit. Furthermore, a portable platform based on **BDP-CHD** was constructed, which has achieved high-throughput discrimination of 16 analytes through linear discriminant analysis (LDA). Moreover, a smartphone adaptable RGB recognition pattern was established for the quantitative detection of multi-analytes. Therefore, this portable fluorescence sensing platform can serve as a versatile tool for rapid and high-throughput detection of toxic phosgene, DCP and volatile acyl chlorides. The proposed "one for more" strategy simplifies multi-target discrimination procedures and holds great promise for various sensing applications.

Phosgene, diethyl chlorophosphate (DCP) and acyl chlorides are essential chemical intermediates, and have been widely used for manufacturing medicines, pesticides, dyes and polymers [1]. It is estimated that tens of thousands of tons of acyl chlorides are consumed globally each year. Whereas, phosgene, DCP and acyl chlorides are highly toxic volatile organic compounds [2]. Exposure to 20 ppm of phosgene can cause severe injury to lung and respiratory in a few minutes, and exposure to 90 ppm phosgene for 0.5 h can be lethal [3,4]. DCP can bind with acetylcholinesterase to inhibit conduction of nerve impulses, leading to organ failure and death within seconds [5-11]. Acetyl chloride can activates the flow of tears as little as 0.5 ppm, and high concentration may cause death or permanent damage [12]. Moreover, most of acyl chlorides can result in dermal and respiratory diseases [13,14-19]. Volatile acyl chlorides pose a serious threat to our public security once industrial leakage accidents happened or they were used as chemical warfare agents (CWAs) by terrorists. To safeguard our public security and human health, it is very important for the development of a simple and efficient tool for on-site high-throughput screening of phosgene, DCP and a diversity of acyl chlorides.

In the past decades, some conventional approaches have been employed to determine phosgene and acyl chlorides, such as gas chromatography, liquid chromatography and electrochemical methods [20-23]. Those methods rely on expensive instruments, which are not suitable for fast security check in subway, airport, railway station and customs due to their poor portability and time-consuming. Fluorescent probes are versatile optical sensors that can generate changes in color and fluorescence signals through host-guest recognition patterns, and has the advantages of high selectivity and sensitivity, low cost and ease of operation [24-27]. A diversity of probes have been devised for sensing of

* Corresponding authors.
E-mail addresses: jianglirong_2000@163.com (L. Jiang), cthniu@163.com (T. Chen), zlt1981@126.com (L. Zeng).
[1] These authors contributed equally to this work.

https://doi.org/10.1016/j.cclet.2024.110222
1001-8417/

phosgene, using different recognition sites, including ethylenediamine, 2-aminoethanol, aldehyde oxime, *o*-phenylenediamino and *o*-hydroxyaniline [28-36]. Likewise, tremendous fluorescent probes were developed for the detection of DCP by utilizing amino, hydroxyl and oxime groups as reaction sites, but some of them give false positive fluorescence signals [37-42]. Whereas, these sensors can only determine one analyte like phosgene or DCP, but neglect diphosgene, acetyl chloride and some other acyl chlorides because these fluorescent probe usually comprise a single luminescent sensor that detect a given analyte *via* the "lock-key "strategy. The array sensing technique inspired by mammalian olfactory/gustatory systems provides a promising solution to address this issue [43,44]. In an array sensing system, multiple independent sensors interact differentially with the target analytes, producing cross-reactive response signals [45]. A distinctive recognition pattern is then generated for each analyte from the signals by processing them through mathematical methods such as linear discriminant analysis (LDA) and principal component analysis, realizing the discrimination of different analytes [46-48]. Nevertheless, in comparison with single-sensor sensing, array sensing requires relatively time-consuming and laborious measurement processes to obtain signal data matrices from multiple sensors. Therefore, it is highly desirable to develop a single fluorescent sensor for high-throughput screening toxic phosgene, DCP and volatile acyl chlorides that are harmful for human health.

Given that fluorescent probe with high-throughput detection performance is particularly attractive: (1) It is a simple but highly efficient manner, (2) more cost-efficient, and (3) it can avoid the spectral cross-talk of multiple sensors, we propose a strategy to sense multiple analytes by using a single fluorescence probe [49-54]. However, it is quite difficult to devise a sensor that can react with multiple analytes and generate different fluorescence signals to high-throughput detect volatile acyl chlorides. 1,2-Diaminocyclohexane (DCH) has two primary aliphatic NH_2 with pKa_1 and pKa_2 of 9.60 and 6.21, respectively. Nucleophilic substitution reaction between NH_2 and acyl chlorides would easily take place in a rapid and effective way. In particular, phosgene would couple with two NH_2 of DCH, which is quite different from some other acyl chlorides. Taking advantage of this feature, in this work, we employed DCH as a reaction site to prepare a "one-for-more" type probe **BDP-CHD** for high-thoughput detection of phosgene, DCP and some other acyl chlorides. DCH was anchored to the *meso*–position of boron dipyrromethene (BODIPY) by nucleophilic substitution with 8-Cl-BODIPY, forming a BODIPY analogue with a C=N double bond. Due to the electron-donating properties of amino group in DCH, photo-induced electron transfer (PET) would happen, which will quench the intrinsic fluorescence of BODIPY core. The adjacent two amino groups in DCH would react with phosgene to form an octahydrobenzimidazolone and BODIPY moiety, giving rise to strong green fluorescence accompanied with chromogenic reaction. Upon exposure to acyl chlorides, the primary aliphatic NH_2 with higher p*K*a would react with acyl chloride or DCP to form amide/phosphamide, which would inhibit the PET course and boasted remarkable blue fluorescence enhancement. Therefore, **BDP-CHD** would realize high-throughput detection of phosgene and other acyl chlorides based on different fluorescence response manners (Scheme 1). Furthermore, a portable sensing platform was constructed by using **BDP-CHD**-loaded melt-blown fabric for high-throughput detection of volatile organic pollutant.

We first investigated the ultraviolet–visible (UV–vis) absorption and fluorescence spectral response of **BDP-CHD** to phosgene and some other acyl chlorides in chloroform. The sensing behavior of **BDP-CHD** to phosgene were assessed by using a non-volatile and low-toxicity counterpart, triphosgene, which can *in situ* generate phosgene in the presence of triethylamine. As shown in Fig. 1a,

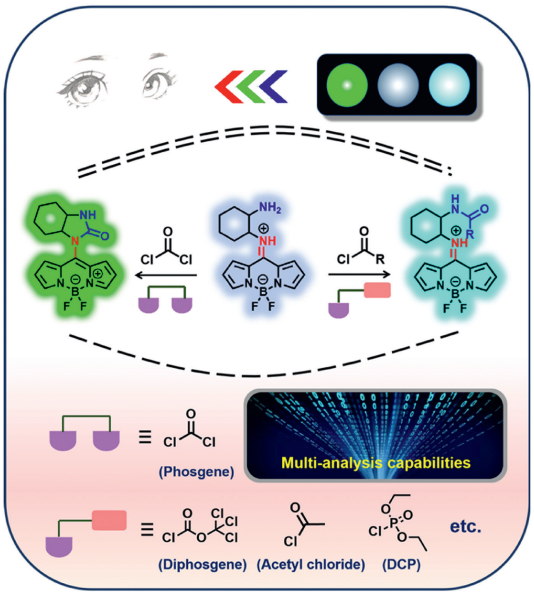

Scheme 1. Schematic illustration of the probe for high-throughput monitoring of phosgene, diphosgene, acyl chlorides and DCP in molecular level.

BDP-CHD displayed a powerful absorption band at 410 nm. After the addition of triphosgene (0–5.0 μmol/L) and triethylamine (TEA), the initial absorption peak (A_{410}) of **BDP-CHD** gradually decreased. Simultaneously, a new absorption peak (A_{500}) increased, and an obvious chromogenic reaction from colourless to yellow was observed (Fig. 1a). The isosbestic point was at 435 nm, indicating that **BDP-CHD** formed a single compound with phosgene. In addition, there was a good linear relationship between the absorbance of **BDP-CHD** and the concentrations of phosgene within the range of 0–2.0 μmol/L ($R^2 = 0.991$) (Fig. 1d). It is noteworthy that the initial absorption band (410 nm) was completely converted to another absorption band (500 nm) after addition of 1.0 equiv. phosgene, implying **BDP-CHD** has high reactivity and sensitivity for phosgene. Subsequently, we explored the fluorescence sensing properties of **BDP-CHD** towards phosgene. **BDP-CHD** exhibited a faint fluorescence band at 476 nm in chloroform ($\Phi_f = 0.12$), which is due to the PET effect from the DCH to the fluorophore (Fig. 1b). After the addition of triphosgene/TEA to the **BDP-CHD** solution, a new fluorescence band at 524 nm ($\Phi_f = 0.46$) emerged. Meanwhile, a clear fluorescence change from weak blue to bright green was observed, which might ascribed to the formation of octahydrobenzimidazolone and BODIPY (Fig. 1b). Furthermore, there was a good linear correlation between the fluorescence intensity of **BDP-CHD** and the concentrations of phosgene within the range of 0–3.0 μmol/L ($R^2 = 0.991$) (Fig. 1e), and an extremely low detection limit (LOD = 51.4 ppt) was obtained, which is sensitive enough to determine trace phosgene from the leakage of industry or accident CWAs terrorist attacks. These findings suggest that **BDP-CHD** could be employed as a ratiometric fluorescent and colormetric dual-mode probe for ultra-sensitive monitoring of phosgene.

We also investigated the spectral response of **BDP-CHD** to acetyl chloride (AC). Upon the addition of AC, the UV–vis absorption spectrum of **BDP-CHD** (5.0 μmol/L) remained silent (Fig. S2 in Supporting information), but a large fluorescence enhancement at 476 nm was observed ($\Phi_f = 0.62$) (Fig. 1c). This observation might be due to the fact that the free aliphatic NH_2 in **BDP-CHD** has reacted with acetyl chloride and the PET process was interrupted. In addition, the fluorescence intensity of **BDP-CHD** had a good linear correlation ($R^2 = 0.991$) with the concentrations of acetyl chloride (Fig. 1f), and the LOD was calculated to be 132.9 ppt (LOD = 3σ/k).

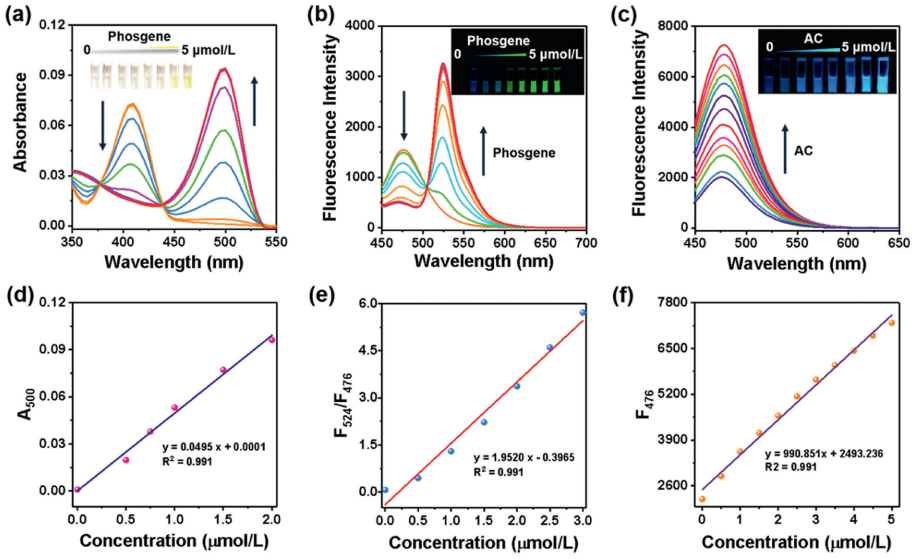

Fig. 1. (a) UV–vis absorption and (b) fluorescence spectra responses of **BDP-CHD** (5.0 μmol/L) to incremental triphosgene (0–5.0 μmol/L)/TEA (100 μmol/L) in chloroform. (c) Fluorescence responses of **BDP-CHD** (5.0 μmol/L) to acetyl chloride (0–5.0 μmol/L) in chloroform. Linear relationship between the (d) absorbance and (e) fluorescence intensity of **BDP-CHD** (5.0 μmol/L) with the concentration of triphosgene/TEA or (f) AC (0–5.0 μmol/L). λ_{ex} = 430 nm, slits: 2.5 nm/5.0 nm.

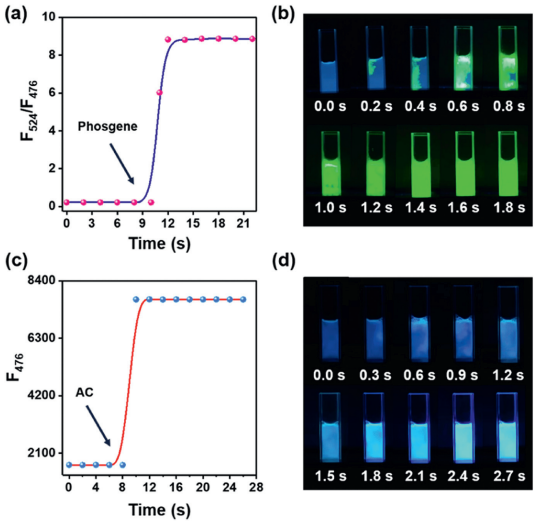

Fig. 2. (a, c) Time-course fluorescence intensity and (b, d) images of **BDP-CHD** (5.0 μmol/L) in $CHCl_3$ containing triphosgene (5.0 μmol/L), TEA (100 μmol/L) or AC (5.0 μmol/L). λ_{ex} = 430 nm, slits: 2.5 nm/5.0 nm.

Based on the above findings, we can conclude that **BDP-CHD** is a highly sensitive fluorescence-enhanced probe that can be used to quantitatively detect acetyl chloride.

Next, we investigated the spectral response of **BDP-CHD** to a wide range of toxic acyl chlorides, such as triphosgene, diphosgene, oxalyl chloride (OC), benzoyl chloride (BzCl), thionyl chloride (TsCl) and DCP, and found that all these acyl chlorides could boast a large fluorescence enhancement at 476 nm (Fig. S3 in Supporting information), which might be ascribed to the high reactivity of free aliphatic NH_2 in **BDP-CHD**. Hence, **BDP-CHD** can act as a high sensitive and general-purpose sensor for high-throughput screening of various acyl chlorides.

For the detection of highly hazardous substances, the response speed of the fluorescent probe should be very fast to reduce the harm to human body. Herein, we explored the response rate of **BDP-CHD** towards phosgene and AC. As shown in Fig. 2a, the ratiometric fluorescence intensity (F_{524}/F_{476}) of **BDP-CHD** reached a plateau within 2 s after the addition of phosgene. Furthermore, we recorded the time-lapse fluorescence images by a live video, as shown in Fig. 2b. The **BDP-CHD** solution showed a faint blue fluorescence under the UV lamp. After the addition of phosgene, a distinct green fluorescence appeared immediately in a local area of the solution, indicating that **BDP-CHD** was able to react rapidly with phosgene. With the diffusion of the phosgene, the entire **BDP-CHD** solution showed an increasing green fluorescence and reached the plateau within 1.6 s. For AC, the fluorescence intensity of **BDP-CHD** at 476 nm reached a maximum within 3 s (Fig. 2c), and the **BDP-CHD** solution showed a distinct blue fluorescence within 2.4 s (Fig. 2d). From these observations, we can conclude that **BDP-CHD** can be used to rapidly detect phosgene and some other violate acyl chlorides.

We then examined the fluorescence response of **BDP-CHD** to phosgene, various acyl chlorides and some potential interfering species, including diphosgene, dimethyl methylphosphonate (DMMP), DCP, TsCl, $POCl_3$, $SOCl_2$, HCl, BzCl, OC, formaldehyde (FA), methylglyoxal (MGO), acrolein, and triphosgene. As shown in Figs. 3a and b, **BDP-CHD** generated a remarkable ratiometric (F_{524}/F_{476}) fluorescence response to phosgene. Diphosgene, DCP and some other acyl chlorides stimulated **BDP-CHD** to produce large fluorescence enhancement at 476 nm, respectively. By contrast, **BDP-CHD** exhibited negligible fluorescence response to the potential interfering species such as hydrochloric acid, DMMP, formaldehyde, methylglyoxal and acrolein, suggesting that **BDP-CHD** has good selectivity for phosgene and acyl chlorides. Given that the different responses of **BDP-CHD** to the above analytes, we conducted a LDA statistical analysis which can identify the optimal linear combinations of features for different classes of analytes. The LDA statistical analysis results were projected on a two-dimensional (2D) space, as shown in Fig. 3c. **BDP-CHD** showed a remarkable green fluorescence after exposed to phosgene. Hence, phosgene itself was divided into a group. Aldehydes, acids, DMMP and **BDP-CHD** cannot lead to significant fluorescence changes, and thus they were divided into another group. Amazingly, acyl chlorides can be categorized into two groups in the LDA diagram according to different fluorescence intensity. These observations demonstrated that **BDP-CHD** can serve as a "one-to-more" probe for high-throughput detection of phosgene, acyl chloride, aldehydes and hydrochloric acid.

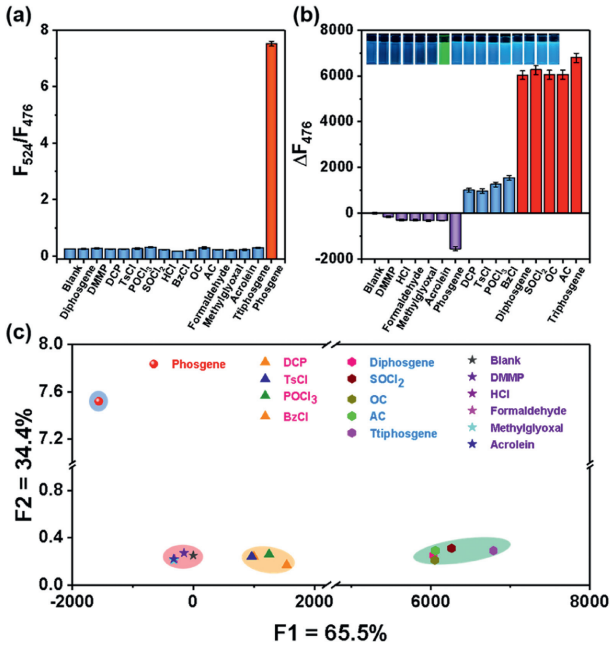

Fig. 3. Fluorescence intensity changes at (a) F_{524}/F_{476} and (b) F_{476} of **BDP-CHD** solution (5.0 μmol/L) upon exposure to various analytes (10.0 μmol/L). (1) Blank, (2) diphosgene, (3) DMMP, (4) DCP, (5) TsCl, (6) $POCl_3$, (7) $SOCl_2$, (8) HCl, (9) BzCl, (10) OC, (11) AC, (12) FA, (13) MGO, (14) acrolein, (15) triphosgene and (16) phosgene. (c) 2D LDA diagram of fluorescent arrays consisting of 16 types of analytes. λ_{ex} = 430 nm, slits: 2.5 nm/5.0 nm. Data are presented as mean ± standard deviation (SD) (n = 3).

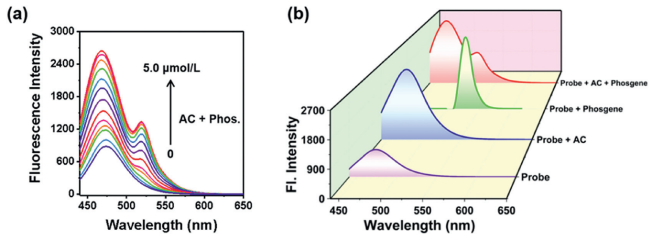

Fig. 4. (a) Fluorescence spectra of **BDP-CHD** solution (5.0 μmol/L) and TEA (100.0 μmol/L) upon the addition of phosgene and AC (0–5.0 μmol/L). (b) Fluorescence spectra of **BDP-CHD** solution (5.0 μmol/L) upon the addition of AC, phosgene or both of AC and phosgene. λ_{ex} = 430 nm, slits: 2.5 nm/5.0 nm.

Given that phosgene and acyl chlorides might co-exist in some cases, herein, we explored the capability of **BDP-CHD** for simultaneous detection of phosgene and AC. After the addition of phosgene and AC, **BDP-CHD** displayed two fluorescence bands at 476 and 524 nm, respectively (Fig. 4a). The fluorescence enhancement at 476 nm was caused by acetyl chloride, and thus can be used to determine acetyl chloride. Another fluorescence band at 524 nm was ascribed to phosgene, which can be utilized to determine phosgene (Fig. 4b). Therefore, **BDP-CHD** not only can discriminate phosgene and acyl chlorides from different emission channels, but also has a good capability for detection of phosgene and acyl chlorides simultaneously.

To explore the working mechanism, we isolated the main product BDP-AC from the reaction mixtures of **BDP-CHD** and acetyl chloride, and tentatively cultured their single-crystals. As shown in Fig. 5a, the bond length between N003 and C007 is 1.322 Å in **BDP-CHD**, implying there is a C=N in **BDP-CHD**. Since **BDP-CHD** exists in the form of BODIPY isomer, it has much shorter UV–vis absorption wavelength and fluorescence wavelength in comparison with ordinary BODIPY core. Besides, **BDP-CHD** exhibited very weak blue fluorescence due to PeT course (Fig. 1). After reaction with acetyl chloride, **BDP-CHD** has transformed to BDP-AC, in which the molecular skeleton of **BDP-CHD** was maintained, but the primary amino group has converted to acetamide. This observation indicated that acetyl chloride has reacted with the primary amine of DCH to form acetamide, which might be reasoned from the fact that the aliphatic primary amine group has much stronger reactivity than tertiary amine (Figs. 5a and b). After reaction with acetyl chloride, the PeT course from amino group to BODIPY core was prohibited. As a result, **BDP-CHD** exhibited a large fluorescence enhancement (Fig. 1c).

We also investigated the working mechanism of **BDP-CHD** for phosgene, and obtained the single crystal of the final reaction product BDP-Phos (Fig. 5a). The single-crystal structure of BDP-Phos showed that phosgene has reacted with the primary amine and the tertiary amine of **BDP-CHD** to form octahydrobenzimidazolone. According to these observations, we proposed the possible working mechanism as following: the primary amine reacted with one chloride of phosgene to form an acetamide, then the adjacent tertiary amine attacked another chloride of phosgene in a nucleophilic addition-elimination reaction. As a result, the DCH group in **BDP-CHD** converted to octahydrobenzimidazolone, and a normal C–N single bond (1.411 Å) was formed, suggesting the probe has transformed to a normal BODIPY core (Fig. 5a). Thus, **BDP-CHD** displayed a remarkable chromogenic reaction along with high contrast green fluorescence response towards phosgene (Figs. 1a and b).

Inspired by the above exciting properties, we would like to fabricate **BDP-CHD** into test strips for on-site screening phosgene and acyl chlorides vapors. Herein, melt-blown fabric was utilized as the matrix for test strips, which would improve the detection efficiency due to their high adsorption capacity. As shown in Fig. 6a, **BDP-CHD** test strips exhibit weak blue fluorescence. After exposure to phosgene (0.5–20 ppm), the original weak blue fluorescence of test strips changed to bright green fluorescence. To determine the accurate concentrations of phosgene and acyl chlorides, we fabricated a portable fluorescence sensing platform that can be used along with a smartphone with a color app to record RGB values of the strips (Fig. 6b). As shown in Fig. 6c, there was a good linear relationship between the ratios of green/blue (G/B) with the concentrations of phosgene in the range of 0–5.0 ppm (R^2 = 0.992), and an obvious fluorescence color change from blue to green was observed from the CIE chromaticity diagram (Fig. 6d). By contrast, acyl chlorides vapors boasted a remarkable blue fluorescence enhancement, and the B values exhibited a good linear correlation (R^2 = 0.994) with the concentrations of acetyl chloride (0–5.0 ppm). The CIE chromaticity coordinates also exhibited notable changes from weak blue to bright blue (Fig. 6e). Therefore, the **BDP-CHD** based sensing platform could be used as a portable detection tool to high-throughput determine the phosgene and volatile acyl chlorides. This portable high-throughput sensing platform is quite practical and superior to traditional instrumental analysis, because it did not rely on large stationary instruments and skilled operators.

To examine the selectivity, **BDP-CHD** test strips were exposed to a variety of analytes vapors, including diphosgene, DMMP, DCP, TsCl, $POCl_3$, $SOCl_2$, HCl, BzCl, OC, AC, FA, MGO, acrolein, triphosgene and phosgene. As shown in Fig. 7a, DMMP, HCl, FA, MGO and acrolein did not cause any fluorescence changes. However, **BDP-CHD** test strips produced bright green fluorescence after exposure to phosgene. By contrast, the test strips exhibited strong blue fluorescence after exposure to DCP and some other acyl chlorides vapors. These significant fluorescence differences can be observed from the CIE chromaticity diagram, and can be used to discriminate phosgene, acyl chlorides and some other analytes (Fig. 7c). Furthermore, we used LDA to analyze the RGB values of **BDP-CHD** test strips after exposure to all these tested analytes, and found that phosgene, acyl chlorides and some other analytes lo-

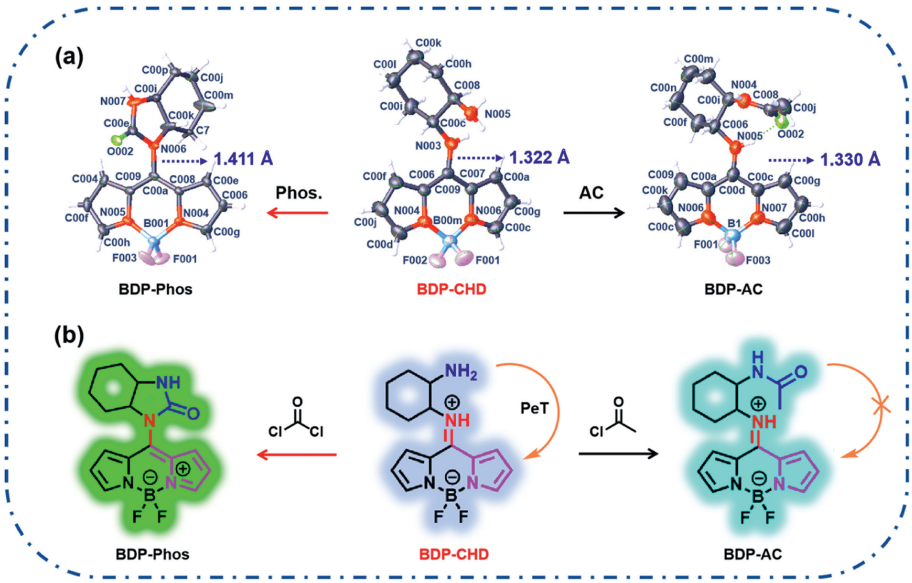

Fig. 5. (a) The single-crystal structure of **BDP-CHD**, BDP-Phos and BDP-AC. (b) The reaction mechanism of **BDP-CHD** with phosgene and acetyl chloride, respectively.

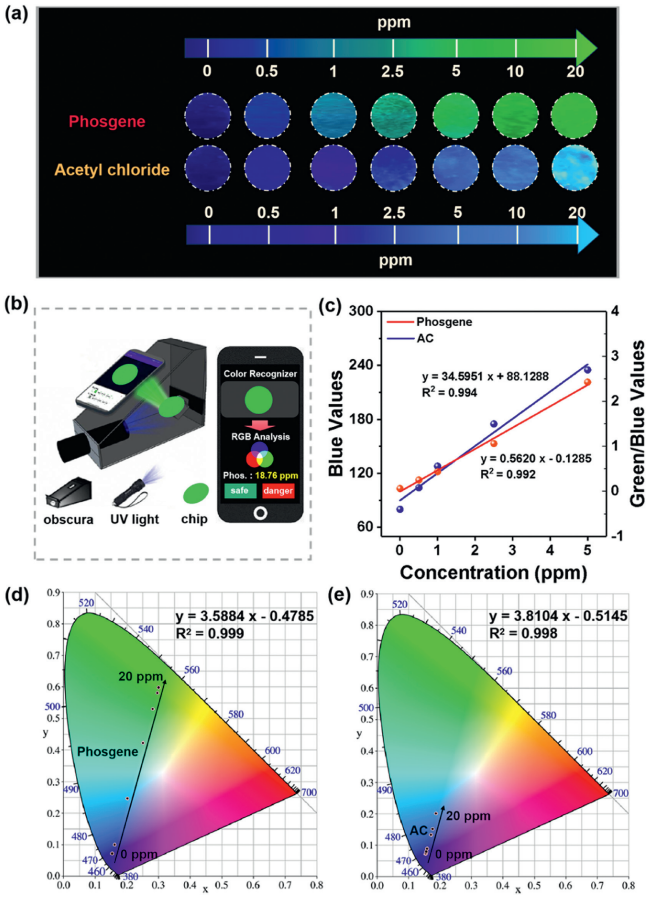

Fig. 6. (a) Fluorescence response images of **BDP-CHD** test strips towards phosgene and acetyl chloride vapor (0–20 ppm). (b) Schematic illustration of fluorescent sensing platform integrated in a smartphone. (c) Linear correlation of the G/B values of strips with phosgene (0–5.0 ppm). Linear correlation of the B values of strips with acetyl chloride vapor (0–5.0 ppm). CIE1931 coordinates of **BDP-CHD** test strips towards incremental (d) phosgene or (e) acetyl chloride (0–20 ppm).

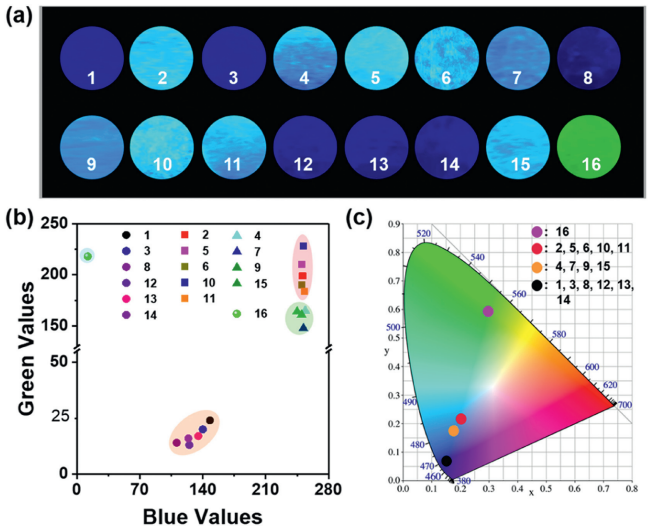

Fig. 7. (a) Fluorescence photographs of **BDP-CHD**-loaded strips upon treatment with phosgene, acyl chlorides or various analytes (20 ppm): (1) blank, (2) diphosgene, (3) DMMP, (4) DCP, (5) TsCl, (6) $POCl_3$, (7) $SOCl_2$, (8) HCl, (9) BzCl, (10) OC, (11) AC, (12) FA, (13) MGO, (14) acrolein, (15) triphosgene, and (16) phosgene. (b) RGB values LDA diagram of **BDP-CHD** test strips for 16 analytes, respectively. (c) CIE1931 coordinates of **BDP-CHD** test strips in the presence of 16 analytes, respectively.

cated at different locations in the 2D LDA diagram (Fig. 7b). These findings indicate that **BDP-CHD** sensing platform can serve as a portable and practical tool for high-throughput screening phosgene and volatile acyl chlorides, and has great potential to be used for security screening in public.

In summary, we have successfully developed a versatile fluorescence platform based on a single molecular probe **BDP-CHD** to realize multiple target analytes sensing and discrimination. **BDP-CHD** reacted with phosgene to form an octahydrobenzimidazolone and BODIPY moiety, giving rise to strong green fluorescence accompanied with chromogenic reaction. By contrast, **BDP-CHD** reacted with acyl chlorides or DCP to form amide/phosphamide, which would inhibit the PET course and boasted remarkable blue fluorescence enhancement. **BDP-CHD** has been fabricated to test strips

that can be used together with smartphone to form a portable intelligent sensing platform. On-site quantitative discriminate detection of multiple analytes has been achieved based on the RGB values of the test strips recorded by smartphone. Thus, this work not only develops a portable fluorescence sensing platform for high-throughput detection of phosgene, DCP and volatile acyl chlorides, but also provides a good strategy to develop sensors for screening multi-analytes.

Declaration of competing interest

The authors declare that they have no known competing financial interests or personal relationships that could have appeared to influence the work reported in this paper.

CRediT authorship contribution statement

Beitong Zhu: Writing – original draft, Methodology, Investigation, Formal analysis. **Xiaorui Yang:** Investigation, Formal analysis. **Lirong Jiang:** Methodology, Investigation. **Tianhong Chen:** Writing – review & editing, Methodology, Conceptualization. **Shuangfei Wang:** Writing – review & editing. **Lintao Zeng:** Writing – review & editing, Supervision, Conceptualization.

Acknowledgment

Acknowledgment for the financial support of the National Natural Science Foundation of China (No. 22168009).

Supplementary materials

Supplementary material associated with this article can be found, in the online version, at doi:10.1016/j.cclet.2024.110222.

References

[1] M.E. Swanson, H.L. Greene, S. Qutubuddin, et al., Appl. Catal. B: Environ. Energy 52 (2004) 91–108.
[2] X. Zhou, Y. Zeng, L. Chen, et al., Angew. Chem. Int. Ed. 55 (2016) 4729–4733.
[3] B. Zhu, R. Sheng, T. Chen, et al., Coord. Chem. Rev. 463 (2022) 214527.
[4] L. Chen, D. Wu, J.M. Kim, et al., Anal. Chem. 89 (2017) 12596–12601.
[5] F. Xiao, D. Lei, C. Liu, et al., Angew. Chem. Int. Ed. 63 (2024) e202400453.
[6] Q. Chen, J. Liu, S. Liu, et al., Anal. Chem. 95 (2023) 4390–4394.
[7] W. Mo, Z. Zhu, F. Kong, et al., Nat. Commun. 13 (2022) 5189.
[8] M. Kumar, N. Kaur, N. Singh, et al., Sensor. Actuat. B: Chem. 392 (2023) 134080.
[9] B. Huo, M. Du, A. Shen, et al., Anal. Chem. 91 (2019) 10979–10983.
[10] L. Zeng, H. Zeng, L. Jiang, et al., Anal. Chem. 91 (2019) 12070–12076.
[11] L. Chen, D. Wu, J. Yoon, ACS Sens. 3 (2018) 27–43.
[12] Q. Wang, H. Wu, A. Gao, et al., Chin. Chem. Lett. 34 (2023) 107644.
[13] T. Chen, L. Jiang, H.Q. Yuan, et al., Sensor. Actuat. B: Chem. 319 (2020) 128289.
[14] X. Yu, L. Fu, T. Wang, et al., Chin. Chem. Lett. 35 (2024) 109167.
[15] G. Yue, S. Su, N. Li, et al., Coordin. Chem. Rev. 311 (2016) 75–84.
[16] W.Q. Meng, A.C. Sedgwick, N. Kwon, et al., Chem. Soc. Rev. 52 (2022) 601–662.
[17] J. Yang, M. Gao, M. Zhang, et al., Coordin. Chem. Rev. 493 (2023) 215289.
[18] N. Couzon, J. Dhainaut, C. Campagne, et al., Coord. Chem. Rev. 467 (2022) 214598.
[19] T. Islamoglu, Z. Chen, M.C. Wasson, et al., Chem. Rev. 120 (2020) 8130–8160.
[20] G.G. Esposito, D. Lillian, G.E. Podolak, et al., Anal. Chem. 49 (1977) 1774–1778.
[21] J. Liu, L. Zhang, W. Zeng, et al., Chin. Chem. Lett. 34 (2023) 108141.
[22] H.B. Singh, D. Lillian, A. Appleby, et al., Anal. Chem. 47 (1975) 860–864.
[23] W. Li, X. Zhang, S. Chen, et al., Chin. Chem. Lett. 33 (2022) 4405–4410.
[24] I. Roy, A. Garci, Y. Beldjoudi, et al., J. Am. Chem. Soc. 142 (2020) 16600–16609.
[25] H. Chen, X. Zeng, H.P. Tham, et al., Angew. Chem. Int. Ed. 58 (2019) 7641–7646.
[26] W. Ren, Y. Zhang, W.Y. Liang, et al., Sensor. Actuat. B: Chem. 330 (2020) 129330.
[27] J. Zhang, C. Yue, Y. Ke, et al., Adv. Agroc. 2 (2023) 127–141.
[28] D. Zhang, L. Wang, X. Yuan, et al., Angew. Chem. Int. Ed. 59 (2019) 695–699.
[29] Q. Hu, C. Duan, J. Wu, et al., Anal. Chem. 90 (2018) 8686–8691.
[30] T.I. Kim, B. Hwang, J. Bouffard, et al., Anal. Chem. 89 (2017) 12837–12842.
[31] H.C. Xia, X.H. Xu, Q.H. Song, ACS Sens. 2 (2016) 178–182.
[32] L. Zeng, H. Zeng, S. Wang, et al., Chem. Commoun. 55 (2019) 13753–13756.
[33] T. Chen, L. Jiang, J.T. Hou, et al., J. Mater. Chem. A 8 (2020) 24695–24702.
[34] X. Liu, N. Li, M. Li, et al., Coordin. Chem. Rev. 404 (2019) 213109.
[35] X. Chen, F. Wang, J.Y. Hyun, et al., Chem. Soc. Rev. 45 (2016) 2976–3016.
[36] Y. Wang, Y. Qin, X. Zhao, et al., Chin. Chem. Lett. 34 (2023) 107576.
[37] S. Bencic-Nagale, T. Sternfeld, D.R. Walt, et al., J. Am. Chem. Soc. 128 (2006) 5041–5048.
[38] T.I. Kim, S.B. Maity, J. Bouffard, et al., Anal. Chem. 88 (2016) 9259–9263.
[39] L. Wang, A. Mei, N. Li, et al., Chin. Chem. Lett. 35 (2024) 108974.
[40] T.J. Dale, J. Rebek, Angew. Chem. Int. Ed. 48 (2009) 7850–7852.
[41] Y.J. Jang, O.G. Tsay, D.P. Murale, et al., Chem. Commun. 50 (2014) 7531–7534.
[42] M.S.J. Khan, Y.W. Wang, M.O. Senge, et al., J. Hazard. Mater. 342 (2017) 10–19.
[43] L. Zheng, R.A. Jon, S.S. Kenneth, Chem. Rev. 119 (2018) 231–292.
[44] L. Zheng, S.S. Kenneth, Acc. Chem. Res. 54 (2020) 950–960.
[45] B. Chen, X. Mo, X. Qu, et al., Anal. Chem. 96 (2024) 6228–6235.
[46] Y. Mei, Q.W. Zhang, Q. Gu, et al., J. Am. Chem. Soc. 144 (2022) 2351–2359.
[47] X. Feng, X. Zhang, J. Huang, et al., Anal. Chem. 94 (2022) 5946–5952.
[48] M. Wu, B. Yang, L. Shi, et al., Anal. Chem. 95 (2023) 3486–4392.
[49] A.J. Pluchinsky, D.J. Wackelin, X. Huang, et al., J. Am. Chem. Soc. 142 (2020) 19804–19808.
[50] X. Gao, S. Li, F. Ding, et al., Angew. Chem. Int. Ed. 58 (2019) 8719–8723.
[51] H. Yan, F. Huo, Y. Yue, et al., J. Am. Chem. Soc. 143 (2020) 318–325.
[52] L. Guo, M. Tian, Z. Zhang, et al., J. Am. Chem. Soc. 143 (2021) 3169–3179.
[53] X. Ma, Y. Huang, W. Chen, et al., Angew. Chem. Int. Ed. 62 (2023) e202216109.
[54] D. Li, T. Shen, X. Xue, et al., Sci. China Chem. 66 (2023) 2329-1338.